

## ESR Study of $V_2O_5$ Catalyst on Carriers

H. TAKAHASHI,\* M. SHIOTANI, H. KOBAYASHI, AND J. SOHMA

*From the Faculty of Engineering, Hokkaido University, Sapporo, Japan*

Received October 2, 1968; revised January 3, 1969

ESR studies were carried out on  $V_2O_5$  catalyst on two different carriers, Neobead and Alundum. The ESR spectrum of  $V_2O_5$  catalyst on the Alundum carrier was a singlet which was similar to the spectrum of pure  $V_2O_5$ . A completely different spectrum having hyperfine structure was obtained from the  $V_2O_5$  catalyst on the Neobead carrier. It was concluded that the ground state of  $V^{4+}$  in the catalyst on the Neobead was the  $d_{xy}$  orbital. The molecular orbital interpretation of the  $g$  factors and the hf coupling constants lead to the conclusion that the unpaired electron was localized on the mother ion  $V^{4+}$ . By computer simulation the linewidths of ESR spectra were determined. The analysis of the ESR spectrum suggests that the  $V^{4+}$  ion in the  $V_2O_5$  catalyst on the Neobead was separately formed. The  $V^{4+}$  ion of  $V_2O_5$  on the Alundum carrier forms a cluster.

### INTRODUCTION

Tarama and his co-workers (1), and other researchers (2, 3), have demonstrated that ESR is a useful technique to obtain information about the local structure surrounding  $V^{4+}$  ion in  $V_2O_5$  catalyst. It was recently found by one of the coauthors (H. K.) that catalytic selectivity of  $V_2O_5$  catalyst for the ammoxidation of toluene to produce benzonitrile was greatly affected by the nature of alumina carriers (4). For instance, when  $V_2O_5$  was dispersed on Neobead carrier the reaction rate of toluene was fairly rapid but the selectivity for benzonitrile was poor and varied over a range of 20%-60% depending on the total conversion, whereas on Alundum carrier it showed fairly high and stable selectivity of 80% but rather lower reaction rates. These results were obtained by careful experiments to avoid the effects of intraparticle diffusion resistance, hence the cause of this difference may be attributed to the nature of carriers. Also the vanadium oxide  $V_2O_{5-\delta}$  on both catalysts during the reaction was analyzed and the values of  $\delta$  were found to be 0-0.05 in the case of the Neobead carrier whereas in the case of the Alundum carrier the value

was in a range as high as 0.2-0.5 under the same reaction conditions. Details on this difference of the catalytic action caused by the carrier will be reported elsewhere by one of the coauthors (5). The present work was undertaken in order to obtain information on whether or not there exist differences in the microstructure of  $V_2O_5$  catalyst depending on the carriers. This paper reports the experimental results of the ESR study of the catalyst on the two different carriers, Alundum and Neobead, and analysis of the ESR spectra obtained from these two systems. Further the difference in the microstructure of  $V_2O_5$  catalyst will be discussed based on the analysis of the ESR spectra.

### EXPERIMENTAL

**Preparation of samples.** A special grade of reagent of  $V_2O_5$  (Kishida Chemical Co.) was used for preparation of catalyst. Neobead carrier (Mizusawa Chemical Co.) was found to be mainly the gel state of alumina by chemical and X-ray analysis.  $V_2O_5$  was dissolved in an aqueous solution of oxalic acid, and, keeping the solution at 100°C, the Neobead carrier was suspended in the solution for 1 hr. The sample of  $V_2O_5$  catalyst on the Neobead carrier was prepared by calcination of the dispersed

\*Deceased.

Neobead at 400°C for 16 hr in an electric furnace. The concentration of  $V_2O_5$  was roughly 5 wt%.

The Alundum carrier (Norton Chemical Co.) is known to be mainly  $\alpha$ -alumina by chemical and X-ray analysis.  $V_2O_5$  catalyst on the Alundum carrier was made in a manner similar to that for the Neobead carrier. The concentration of  $V_2O_5$  was also roughly 5 wt%.

**ESR measurements.** The ESR spectrometer used was a JEOL† 3-BX, in which microwave frequency was the X band and 100 kc/sec modulation was adopted. The static magnetic field was calibrated with the standard sample of  $Mn^{2+}$  supplied by JEOL. All measurements were done in air at room temperature. ESR measurements were carried out for three samples: pure  $V_2O_5$ ,  $V_2O_5$  on Neobead, and  $V_2O_5$  on Alundum. In order to detect changes in the spectra caused by the ammoxidation reaction, the ESR spectra were observed for the same sample before and after the reaction. Since the reaction had been conducted at elevated temperatures, the samples were cooled down to room temperature in an  $N_2$  atmosphere.

### RESULTS

Pure  $V_2O_5$  showed a singlet spectrum, of which the  $g$  factor was 1.98 and the linewidth expressed by maximum slope separation,  $\Delta H_{msl}$ , was 85 G. The line shape was nearly Lorentzian. This spectrum agreed with that observed by Tarama and his co-workers (1). This spectrum has been attributed by various researchers to  $V^{4+}$  ion, which exists in the nonstoichiometric compound  $V_2O_{5-\delta}$  formed by partial reduction. The spectra from the  $V_2O_5$  on Alundum carrier was observed as singlet which had the same  $g$  factor of 1.98 but variable linewidth from 30 G to 120 G in  $\Delta H_{msl}$ . The line shape was also Lorentzian, as shown in Fig. 1. Both the line shape and the  $g$  factor were unvaried before and after the reaction, but the intensity was increased after reaction. A resonance band other than the  $g = 1.98$  band was observed in the samples with carriers. This extra absorption band pre-

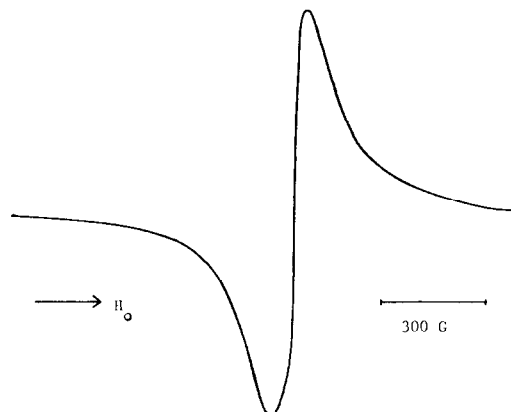


FIG. 1. ESR spectrum of the  $V_2O_5$  catalyst on Alundum carrier: after reaction.

sumably arises from  $Fe^{3+}$  ion, an impurity in the alumina. In our studies this extra band was disregarded because the impurity in the carriers apparently does not play an important role in the catalytic action of  $V_2O_5$ . A completely different spectrum was observed for the  $V_2O_5$  on Neobead carrier, as shown in Fig. 2. Spectrum (a) in Fig. 2 is that obtained from the sample before reaction and the spectrum (b), that after reaction.

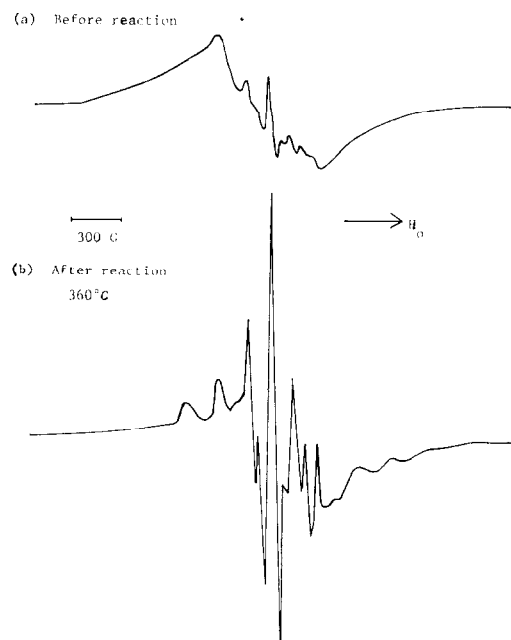


FIG. 2. ESR spectra of the  $V_2O_5$  catalyst on Neobead carrier: (a) before reaction; (b) after reaction.

† Japan Electron Optics Laboratory.

### Spectrum of $V_2O_5$ on Neobead Carrier

The spectrum obtained for the  $V_2O_5$  catalyst on Neobead after reaction showed most clearly the hyperfine structure caused by the nuclear magnetic moment of vanadium, as shown in Fig. 2(b). More than 99% of the natural abundance of V is  $^{51}\text{V}$  and its nuclear moment is  $\frac{7}{2}$ . Thus octet is the expected hyperfine structure of the vanadium spectrum, but anisotropies of both the  $g$  factor and the hyperfine coupling constant complicate a spectrum obtained for an amorphous sample like ours. Analysis of the complicated spectrum, shown in Fig. 2(b), was successfully guided by the method developed by Hecht and Johnston (6). The spectrum was analyzed using an axial symmetric spin Hamiltonian (7)

$$\mathcal{H} = \beta(g_{\parallel}H_xS_x + g_{\perp}H_xS_x + g_{\perp}H_yS_y) + A_{\parallel}S_zI_z + A_{\perp}S_xI_x + A_{\perp}S_yI_y \quad (1)$$

where  $\beta$  is the Bohr magneton,  $g_{\parallel}$  and  $g_{\perp}$  are the parallel and perpendicular principal components of the  $g$  tensor;  $A_{\parallel}$  and  $A_{\perp}$  are the parallel and perpendicular principal components of the hyperfine-coupling tensor;  $H_x$ ,  $H_y$ ,  $H_z$  are the components of the magnetic field;  $S_x$ ,  $S_y$ ,  $S_z$  and  $I_x$ ,  $I_y$ ,  $I_z$  are the components of spin operators of the electron and nucleus, respectively, and the coordinate system is fixed to the molecule. The absorption peaks are related to  $2I + 1$  values of  $m$ , and the peaks occur at the field of

$$H_{\parallel} = 2H_0/g_{\parallel} - (A_{\parallel}/g_{\parallel}\beta)m \quad (\text{for } \theta = 0) \quad (2)$$

$$H_{\perp} = 2H_0/g_{\perp} - (A_{\perp}/g_{\perp}\beta)m \quad (\text{for } \theta = \pi/2) \quad (3)$$

where  $\theta$  is the angle spanning between  $H_0$  and the axial symmetry axis of the ion site. Plotting the magnetic field of the observed peaks corresponding to either  $H_{\perp}$  or  $H_{\parallel}$  against the nuclear quantum number  $m$ , one can obtain a linear relation, as shown in Fig. 3. The slopes and the intercepts with the  $m_I = 0$  line can be used to derive values of the desired parameters,  $g_{\parallel}$ ,  $A_{\parallel}$ ,  $g_{\perp}$ , and  $A_{\perp}$ . Assignment of the peaks of the observed spectrum was attained by this analysis and is illustrated as two sets of octets as shown in Fig. 4. Table 1 lists the numerical values

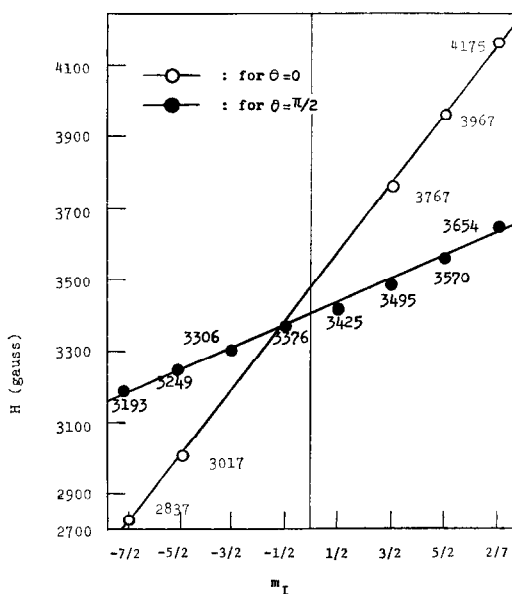


FIG. 3. Magnetic field vs. nuclear quantum number.

of the parameters determined by this analysis.

### Simulation of the Spectra

The samples used in these experiments were of either amorphous or polycrystalline state. The line shape for either the amorphous or the polycrystalline state was theoretically derived by Neiman and Kivelson (8). Based on their expression and an assumption of a Gaussian line shape of each component, computer simulations were carried out by NEAC 2203 G. In the simulations the parameters listed in Table 1 were used and the linewidth expressed by dispersion values  $\langle \Delta H^2 \rangle$  of Gaussian was chosen as the adjustable parameter. The pattern shown in Fig. 5 was found to be best fitted by the observed one shown in Fig. 4. Two patterns, the observed and the best simulated, coincide with each other on major characteristics, such as number and relative intensities of the peaks. The linewidth which gave the best simulated pattern was 50 G. As the linewidth as the variable parameter in the simulation was increased, the resolution of the spectra was decreased, as demonstrated in Fig. 6. The broader

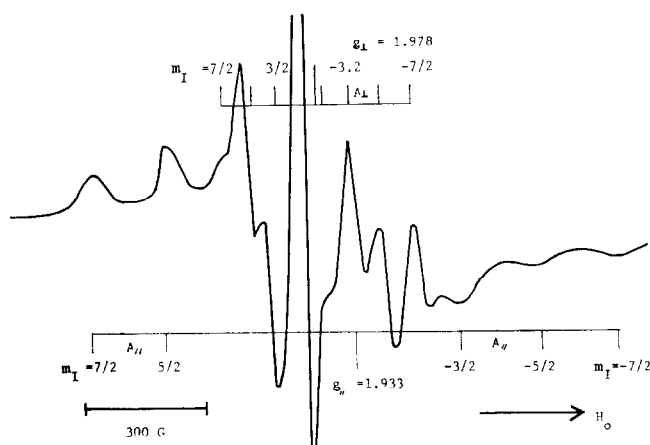


FIG. 4. Assignment of each peak in the spectrum of V<sub>2</sub>O<sub>5</sub> catalyst on Neobead carrier.

linewidth than 300 G smeared out the resolved spectrum and gave a broad singlet. The separation between maximum slope was 660 G in the broad singlet.

#### *Symmetry Property of Local Field Surrounding V<sup>4+</sup> Ion in the Catalyst*

It is well known that anisotropy of the  $g$  factor depends on the spin-orbit coupling constant  $\lambda$  and splitting of the energy levels of the paramagnetic ion caused by the local crystalline field surrounding a paramagnetic ion (9, 10). The symmetry properties of the crystalline field about a paramagnetic ion determine separation of the energy levels of the ion by removing the degenerated energy states of a free ion and cause an anisotropy of the  $g$  factor. The detailed analysis of the anisotropy of the observed  $g$  factor was presented by Hecht for V<sup>4+</sup> in V<sub>2</sub>O<sub>5</sub> and the local symmetry about V<sup>4+</sup> ion was clearly determined (6). Using a procedure similar to Hecht's analysis from the observed anisotropy of the  $g$  factor it was possible to determine the local symmetry of the field surrounding V<sup>4+</sup> ion in the V<sub>2</sub>O<sub>5</sub> catalyst.

The observed components of the  $g$  factor, which are tabulated in Table 1, show that the  $g$  tensor of V<sup>4+</sup> ion has axial symmetry and the parallel component,  $g_{\parallel} = g_{zz} = 1.933$ , is smaller than the perpendicular ones,  $g_{\perp} = g_{xx} = g_{yy} = 1.997$ . By using the reasonable experimental values of the energy gap between the first excited state and the ground state of the V<sup>4+</sup> ion, which were the same values taken by previous researchers (6, 11, 12), a theoretical discussion similar to Hecht's leads us to the conclusions that the symmetry of the field about V<sup>4+</sup> is uniquely determined to be fourfold, either  $D_{4h}$  or  $C_{4v}$ , and the  $d_{xy}$  orbital is the ground state of the V<sup>4+</sup> ion in this symmetry.

#### *Molecular Orbital Interpretation of ESR Parameters*

As shown in the former section, it is concluded by the analysis of the  $g$  tensor that either  $C_{4v}$  or  $D_{4h}$  is the symmetry around the V<sup>4+</sup>. The IR spectrum (13) and crystallographic data (14) of V<sub>2</sub>O<sub>5</sub> showed that two oxygen atoms situated on the fourfold

TABLE 1  
SPIN HAMILTONIAN PARAMETERS OF THE SPECTRUM OF V<sub>2</sub>O<sub>5</sub> ON THE NEOBEAD CARRIER<sup>a</sup>

$ A_{\parallel} $	$ A_{\perp} $	$ A_0 $	$g_{\parallel}$	$g_{\perp}$	$g_0$	$H_{\parallel} (m_I = 0)$	$H_{\perp} (m_I = 0)$
$170 \times 10^{-4} \text{ cm}^{-1}$ 189 G	$61 \times 10^{-4} \text{ cm}^{-1}$ 66 G	$(97 \times 10^{-4}) \text{ cm}^{-1}$ (107) G	1.933	1.978	(1.963) <sup>a</sup>	3500 G	3420 G

<sup>a</sup> ( ) indicates calculated values.

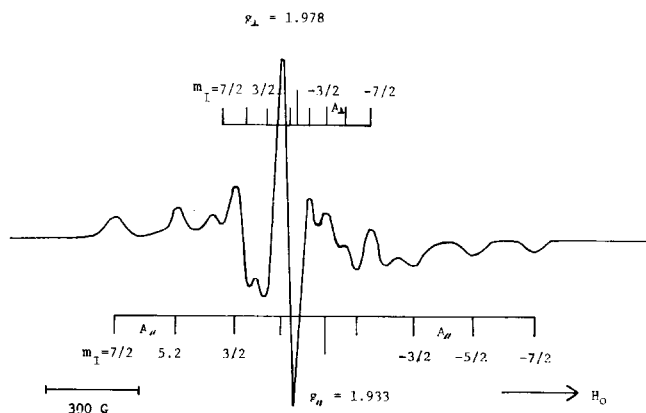


FIG. 5. Computer-simulated ESR spectrum. The parameters tabulated in Table 1 were used and the linewidth was taken as adjustable parameter in the computation. For this spectrum the linewidth was chosen as 50 G.

symmetry axis are not equivalent with respect to the central  $V^{5+}$  ion. Thus,  $D_{4h}$  symmetry is ruled out and  $C_{4v}$  symmetry fits the facts. The molecular orbitals of the vanadium complex having  $C_{4v}$  symmetry are essentially the same as those employed by previous workers (6, 11, 12). The antibonding orbitals are obtained by replacing the unprimed coefficients by their starred counterparts and the primed coefficients by the negative starred ones in the following equations:

$$\begin{aligned}
 \Phi^*(b_{2g}) &= \beta_2^* 3d_{xy} - \beta_2'^*(1/2)(p_{y1} + p_{x2} - p_{y3} - p_{x4}) \\
 \Phi^*(b_{1g}) &= \beta_1^* 3d_{x^2-y^2} - \beta_1'^*(1/2) \times (\sigma_1 - \sigma_2 + \sigma_3 - \sigma_4) \\
 \Phi^*(e_\pi) &= \xi_\pi^* 3d_{xy} - \xi_\pi'^* p_{x5} \\
 &= \xi_\pi^* 3d_{yz} - \xi_\pi'^* p_{y5} \\
 \Phi^*(e_\sigma) &= \xi_\alpha^* 4p_x - \xi_\alpha'^*(1/\sqrt{2})(\sigma_1 - \sigma_3) \\
 &= \xi_\alpha^* 4p_y - \xi_\alpha'^*(1/\sqrt{2})(\sigma_2 - \sigma_4) \\
 \Phi^*(a_1) &= \alpha_1^*(1/\sqrt{2})(4s + 3d_{z^2}) - \alpha_1'^* \sigma_5 \\
 \Phi^*(a_1) &= \alpha_2^*(1/\sqrt{2})(4s - 3d_{z^2}) - \alpha_2'^*(1/2)(\sigma_1 + \sigma_2 + \sigma_3 + \sigma_4) \\
 \Phi^*(a_1) &= \alpha_3^* 4p_z - \alpha_3'^* \sigma_6
 \end{aligned} \tag{4}$$

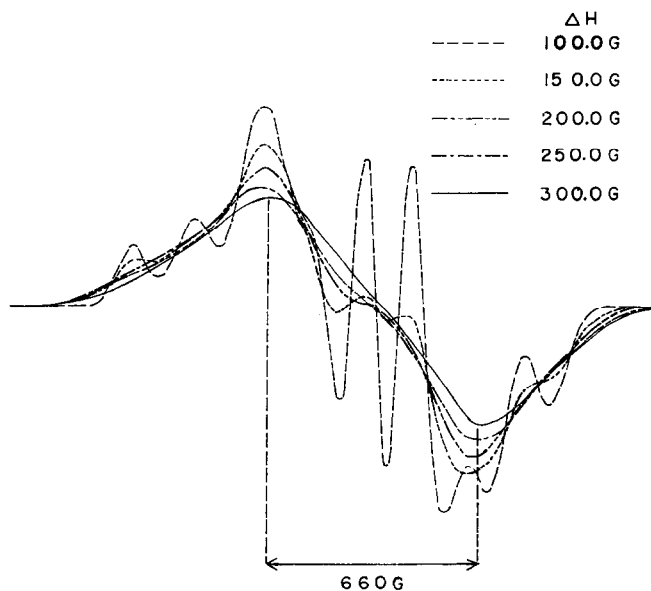


FIG. 6. Various simulated patterns obtained by changing the linewidth,  $\Delta H$ .

where  $\sigma_i$ ,  $p_{xi}$ , and  $p_{yi}$  are the  $sp^2$ ,  $2p_x$ , and  $2p_y$  orbitals of the  $i$ th ligand directed to the central V<sup>4+</sup>, respectively. Eighteen electrons occupy nine bonding orbitals and an unpaired electron exists on the lowest antibonding level  $\Phi^*$  ( $b_{2g}$ ) ( $6$ ). The following equations connecting the molecular orbital parameters  $\beta_2^*$  with the coupling constants  $A_{\parallel}$  and  $A_{\perp}$  were derived by the various authors ( $6$ ,  $12$ ,  $15$ ):

$$A_{\parallel} = P \left\{ -\beta_2^{*2} \left( \frac{2}{3} + K \right) + (g_{\parallel} - 2.002) + \frac{2}{3} (g_{\perp} - 2.002) + D_{\parallel} + \frac{2}{3} D_{\perp} \right\} \quad (5)$$

$$A_{\perp} = P \left\{ \beta_2^{*2} \left( \frac{2}{3} - K \right) + \frac{1}{4} (g_{\perp} - 2.002) + \frac{1}{4} D_{\perp} \right\} \quad (6)$$

In Eqs. (5) and (6),  $A_{\parallel}$ ,  $A_{\perp}$ ,  $g_{\parallel}$ , and  $g_{\perp}$  were experimentally obtained.  $P$  and  $K$  in the above equation is defined by the equations

$$K = \frac{(6/7)(A_{\parallel} + 2A_{\perp}/3)}{A_{\parallel} - A_{\perp}} \quad (7)$$

$$P = -(A_{\parallel} + 2A_{\perp}/3)/K \quad (8)$$

$P$  and  $K$  were evaluated from the experimental data. Thus, it is possible to evaluate experimentally the value of  $\beta_2^*$ ; it was found to be unity. In this estimation the values given by Kivelson were used for  $D_{\parallel}$  and  $D_{\perp}$  ( $12$ ). One could evaluate further the coefficient of the other  $\sigma$  molecular orbital,  $\beta_1^*$ , and the coefficient of the  $\pi$ -orbital,  $\xi_1^*$ , after the manner of Kivelson ( $12$ ). The numerical values taken in this evaluation were the same as those in Kivelson's paper for the energy gaps  $\Delta E_{x^2-y^2}$  and  $\Delta E_{zz}$ , the spin-orbit coupling,  $\lambda$ , and the overlap integrals  $S$  and  $\pi_0$ , because as a first approximation these values may be assumed to be those used by Kivelson. The values for  $\beta_1^*$  and  $\xi_1^*$  estimated by the procedures mentioned above are listed in Table 2. It is

TABLE 2  
MOLECULAR PARAMETERS FOR NEOBEAD-SUPPORTED V<sub>2</sub>O<sub>5</sub><sup>a</sup>

$K$	$P$	$\beta_2^{*2}$	$\beta_1^{*2}$	$\xi_1^{*2}$
0.774	$125 \times 10^{-4}$ cm <sup>-1</sup>	1	(0.98)	(0.96)

<sup>a</sup> ( ) indicates that in order to determine  $\beta_1^{*2}$  and  $\xi_1^{*2}$   $\Delta E_{x^2-y^2} = 17\,000$  cm<sup>-1</sup> and  $\Delta E_{zz} = 14\,000$  cm<sup>-1</sup> were used, respectively.

worth mentioning that the molecular orbital coefficients of vanadium ions,  $\beta_2^*$ ,  $\beta_1^*$ , and  $\xi_1^*$  are all either unity or close to unity. This means that the nature of chemical bonding between V<sup>4+</sup> ion and oxygen atoms is ionic and the unpaired electron originating from vanadium ion is localized on its mother ion.

### Linewidth

It is impossible by measuring separations between maxima and minima of the spectrum to estimate directly the linewidth of such a complicated spectrum as the V<sup>4+</sup> spectrum obtained from an amorphous sample. As mentioned in the former section one can simulate an experimental spectrum by use of an electronic computer, choosing the linewidth as an adjustable parameter. In this simulation the value of the linewidth which gives the simulated spectrum closest to the experimental one is taken as a kind of experimental value of the linewidth. The experimental value of the linewidth determined by the computer simulation was 50.0 G for the observed spectrum of V<sub>2</sub>O<sub>5</sub> on the Neobead carrier, as shown in the former section. Although there are various factors affecting the linewidth of the ESR spectrum, the magnetic dipole-dipole interaction in this case is reasonably assumed to be the major factor. In other words it is assumed that the local field produced by the nearest neighbor V<sup>4+</sup> ion contributes mainly to the linewidth. Since the samples were amorphous the angular contribution of the local field was averaged out and the linewidth due to the dipolar local field depended merely on the distance and was given by Anderson and Weiss ( $16$ ) by the following equation:

$$\Delta H_p = (g_0 \beta_0 / r^3) [5.1 S(S+1)]^{1/2} \quad (9)$$

where linewidth  $\Delta H_p$  is expressed by the half-width;  $r$  is the distance to the nearest neighbor; and  $S$  is the spin quantum number. Inserting the experimental value of 50.0 G for  $\Delta H_p$  in the above equation, the distance to the nearest neighbor was estimated as 9.15 Å. From the analysis of linewidth it is concluded that the V<sup>4+</sup> ions of the V<sub>2</sub>O<sub>5</sub> catalyst on the Neobead carrier are separated by nearly 9 Å from each other.

*Spectrum of V<sub>2</sub>O<sub>5</sub> Catalyst on the Alundum Carrier*

As shown in Fig. 1, the spectrum of V<sub>2</sub>O<sub>5</sub> on the Alundum carrier was a singlet, the linewidth of which varied depending on the treatment. The molecular orbital analysis of the spectrum of V<sub>2</sub>O<sub>5</sub> on the Neobead carrier leads us to the conclusion that the unpaired electron is localized on the V<sup>4+</sup> ion. Thus the hyperfine structure due to the nuclear magnetic moment of V<sup>4+</sup> should appear in the spectrum of V<sub>2</sub>O<sub>5</sub> on the Alundum instead of the observed structureless singlet. One may reasonably assume in this case that broadening of spectral lines reduces the resolution of the spectrum so much as to smear out the structure. As shown in the computer-simulated spectra, the linewidth of 300 G was broad enough to give a broad singlet and the apparent linewidth of the superposed singlet is 660 G, as shown in Fig. 6. However, the observed separation between maximum and minimum of the derivative of the singlet was much narrower than 660 G and the observed line shapes were Lorentzian. The Lorentzian line shape suggests the existence of a narrowing mechanism, such as motional narrowing or exchange narrowing. One can hardly imagine motional narrowing in the solid sample. Thus, exchange is the plausible mechanism to narrow the linewidth caused by dipole-dipole interaction. According to Anderson and Weiss (16) the linewidth narrowed by exchange is given by the following equation:

$$\Delta H = \frac{1}{3} \frac{H_p^2}{H_e} \quad (10)$$

where  $H_e$  is the exchange frequency expressed in terms of the magnetic field. In Eq. (10)  $\Delta H_p$  is expected to be broad enough to mask the hyperfine structure, that is, larger than 300 G. The distance between the nearest dipoles which give a linewidth of more than 300 G is estimated by Eq. (9) to be less than 5.03 Å. A distance less than 5 Å probably can not exclude the exchange-narrowing due to electron exchange. Thus the exchange may occur among such close neighbors. The argument presented above leads us to consider that the V<sup>4+</sup> ions in the V<sub>2</sub>O<sub>5</sub> catalyst on the Alundum carrier were formed

close enough to each other to produce dipolar broadening and exchange-narrowing. In other words the narrowed singlet of the V<sup>4+</sup> spectrum suggests that the V<sup>4+</sup> impurity occurs in microscopically dense clusters and that the clusters may be dispersed evenly in the sample.

#### DISCUSSION

By the BET method the surface area of Neobead was found to be nearly 40 times larger than that of Alundum (3). It was found that, in the samples used in these experiments, V<sub>2</sub>O<sub>5</sub> occupied merely about a quarter of the total surface area of Neobead carrier while V<sub>2</sub>O<sub>5</sub> covered with about eight layers the total surface area of the Alundum carrier. Thus, as a first approximation, the environment around a molecule of V<sub>2</sub>O<sub>5</sub> on Alundum carrier is considered to be the same as pure V<sub>2</sub>O<sub>5</sub>. This approximation is supported by the fact that the ESR spectrum of V<sub>2</sub>O<sub>5</sub> on the Alundum carrier was the same that of V<sub>2</sub>O<sub>5</sub>. In stoichiometric V<sub>2</sub>O<sub>5</sub> the electric charge neutrality holds in each unit cell. Suppose a single vanadium ion is reduced from V<sup>5+</sup> to V<sup>4+</sup> in this stoichiometric V<sub>2</sub>O<sub>5</sub>. The neutrality in the unit cell, in which reduction occurs, is now broken and thus the reduction of one ion may be unstable. However, if two vanadium ions existing in two neighboring unit cells are reduced and one oxygen atom shared by the two unit cells is simultaneously removed, the charge neutrality is again recovered because two positive charges compensate with two negative charges of the oxygen. That is, the formation of two neighboring V<sup>4+</sup> ions is more stable than two separate V<sup>4+</sup> ions. Therefore one is led to believe that V<sup>4+</sup> ions may be formed not separately but in a cluster. This charge neutrality discussion seems to present a mechanism for the cluster formation of V<sup>4+</sup> which was derived in the former section from the spectra of V<sub>2</sub>O<sub>5</sub> catalyst on the Alundum carrier. The distance between two neighbor V<sup>4+</sup> ions was estimated to be less than 5 Å and this distance of 5 Å is close to the distance between two V<sup>4+</sup> ions in the neighboring unit cells, nearly 4 Å (1, 14). On the other hand the V<sub>2</sub>O<sub>5</sub> catalyst on the Neobead

carriers was a monolayer and the coverage by the catalyst was merely 25% of the total surface area. Thus the approximation to crystalline structure of pure V<sub>2</sub>O<sub>5</sub> does not hold for this sample. The cluster formation of V<sup>4+</sup> ions is not expected for the V<sub>2</sub>O<sub>5</sub> on the Neobead carrier and V<sup>4+</sup> may be formed rather dispersedly to give the well-resolved ESR spectrum.

#### ACKNOWLEDGMENT

The authors should like to express their cordial thanks to Mr. S. Moriuchi for his cooperation of carrying out the computer simulation.

#### REFERENCES

1. TARAMA, K., TERANISHI, S., YOSHIDA, S., AND TAMURA, N., *Proc. Intern. Congr. Catalysis, 3rd, Amsterdam, 1964*, p. 282. North-Holland Publ. Co., 1965.
2. JOFFE, J., *et al.*, *Kinetica i Kataliz* **5**, 861 (1964).
3. HIROTA, K., AND KUWATA, K., *Bull. Chem. Soc. Japan* **36**, 229 (1963).
4. TANABE, H., ARAI, F., AND KOBAYASHI, H., *5th Symposium of Reaction Engineering (Tokyo)*, p. 61. Soc. Chem. Eng. Japan, (1965).
5. KOBAYASHI, H., *et al.*, *Shokubai (Tokyo)* **10**, 92 (1968).
6. HECHT, H. G., AND JOHNSTONE, T. S., *J. Chem. Phys.* **46**, 23 (1967).
7. BLEANEY, B., *Phil. Mag.* **42**, 441 (1951).
8. NEIMAN, R., AND KIVELSON, D., *J. Chem. Phys.* **35**, 156 (1961).
9. PRYCE, M. H. L., *Proc. Phys. Soc. (London)* **A63**, 25 (1950).
10. BALLHAUSEN, C. J., "Introduction to Ligand Field Theory." McGraw-Hill, New York, 1962.
11. BALLHAUSEN, C. J., AND GRAY, H. B., *Inorg. Chem.* **1**, 11 (1962).
12. KIVELSON, D., AND LEE, S. K., *J. Chem. Phys.* **41**, 1896 (1964).
13. YOKOYAMA, S., Master's Thesis, Faculty of Engineering, Hokkaido Univ., Japan.
14. BYSTROM, A., *et al.*, *Acta. Chem. Scand.* **4**, 1119 (1950).
15. ABRAGAM, A., AND PRYCE, M. H. L., *Proc. Roy. Soc. (London)* **A205**, 135 (1951).
16. ANDERSON, P. W., AND WEISS, T. R., *Rev. Mod. Phys.* **25**, 1269 (1953).